

## SNX10 is Required for Osteoclast Formation and Resorption Activity

C.H. Zhu,<sup>1</sup> L. R. Morse,<sup>1,2</sup> and R. A. Battaglini<sup>1\*</sup>

<sup>1</sup>Department of Cytokine Biology, Forsyth Institute, Boston, Massachusetts

<sup>2</sup>Department of Physical Medicine and Rehabilitation, Harvard Medical School and Spaulding Rehabilitation Hospital, Boston, Massachusetts

### ABSTRACT

RANKL-stimulation of osteoclast precursors results in up-regulation of genes involved in the process of differentiation and activation. In this report we describe the expression and functional characterization of *Sorting Nexin 10* (*snx10*). Snx10 belongs to the sorting nexin (SNX) family, a diverse group of proteins with a common feature: the PX domain, which is involved in membrane trafficking and cargo sorting in endosomes. *Snx10* is strongly up-regulated during RANKL-induced osteoclast differentiation in vitro and expressed in osteoclasts in vivo. qPCR analysis confirmed a significant increase in the expression of *snx10* in in vitro-derived osteoclasts, as well as in femur and calvaria. Immunohistochemical analysis of mouse embryo sections showed expression in long bone, calvariae, and developing teeth. The expression was limited to cells that also expressed TRAP, demonstrating osteoclastic localization. Confocal immunofluorescence and subcellular fractionation analysis revealed Snx10 localization in the nucleus and in the endoplasmic reticulum (ER). To study a possible role for *snx10* in osteoclast differentiation and function we silenced *snx10* expression and found that *snx10* silencing inhibited RANKL-induced osteoclast formation and osteoclast resorption on hydroxyapatite. Silencing also inhibited TRAP secretion. Taken together, these results confirm that *snx10* is expressed in osteoclasts and is required for osteoclast differentiation and activity in vitro. Since inhibition of vesicular trafficking is essential for osteoclast formation and activity and SNX10 is involved in intracellular vesicular trafficking, these studies may identify a new candidate gene involved in the development of human bone diseases including osteoporosis. *J. Cell. Biochem.* 113: 1608–1615, 2012. © 2011 Wiley Periodicals, Inc.

**KEY WORDS:** OSTEOCLAST; BONE RESORPTION; SORTING NEXIN; VESICULAR TRAFFICKING

**B**one resorption is regulated by a complex system of hormones and cytokines that cause osteoblasts/stromal cells and lymphocytes to produce factors like RANKL, which ultimately result in the differentiation and activation of osteoclasts. Osteoclasts, the bone resorbing cells, are multinucleated cells of the monocyte-macrophage lineage that form by differentiation and fusion of mononuclear precursors.

Osteoclasts are exceptionally dependent on vesicular trafficking to form the ruffled border, a process essential for bone resorption. Consequently, disruption (genetic or pharmacological) of osteoclastic vesicle transport abolishes cellular resorptive activity [Coxon and Taylor, 2008]. Transcytosis of endocytosed material is essential for cellular activity and has been observed in osteoclasts [Stenbeck and Horton, 2004]. Bone resorption by osteoclasts involves the following cellular events: (1) adhesion and migration, which is dependent upon rapid assembly and disassembly of cytoskeleton proteins at

sites of adhesion; (2) secretion of proteolytic enzymes, dependent upon vesicular transport to the secretory ruffled border; (3) internalization, or transcytosis, of vesicles from the ruffled border to the lysosomes via vesicular transport in a retrograde manner; and (4) acidification via the apical vacuolar proton ATPase and the Cl<sub>7</sub> chloride channel at the ruffled border membrane and homeostatic ion transport at the basolateral membrane [Baron and Horne, 2005]. Vacuolar and vesicular transport functions are key to all these processes.

The sorting nexin (SNX) family of proteins consists of a diverse group of cytoplasmic and membrane-associated proteins involved in various aspects of endocytosis and protein trafficking [Worby and Dixon, 2002]. These proteins are unified by a common phospholipids-binding motif (the PX domain), which enables them to form protein–protein complexes and protein–lipid interactions in protein sorting and membrane trafficking [Worby and Dixon,

\*Correspondence to: R. A. Battaglini, PhD, Department of Cytokine Biology The Forsyth Institute 245 First Street Cambridge, MA 02142. E-mail: rbattaglini@forsyth.org

Received 1 May 2011; Accepted 5 December 2011 • DOI 10.1002/jcb.24029 • © 2011 Wiley Periodicals, Inc.

Published online 15 December 2011 in Wiley Online Library (wileyonlinelibrary.com).

2002]. PX-containing proteins also are involved in vacuole sorting in yeasts, suggesting that SNXs can regulate membrane trafficking and cargo sorting in endosomes.

SNX10 belongs to the SNX family. This protein can induce formation of giant vacuoles in transfected cells and may be involved in the regulation of endosome homeostasis [Qin et al., 2006]. We found SNX10 to be induced by RANKL stimulation *in vitro*. The goal of this study was to characterize expression and function of *snx10* during osteoclast differentiation.

## MATERIALS AND METHODS

### ANIMALS

All animal studies were approved by the Institutional Animal Care and Use Committee at our institution and were in compliance with all federal and local guidelines. All mice were of the 129/C57 mixed background.

### CELLS

RAW 264.7 (TIB-71) mouse macrophage/monocytes were purchased from ATCC. Cells were cultured in DMEM/1.5 g/l sodium bicarbonate (JRH Biosciences, Lenexa, KS) supplemented with 10% nonheat inactivated FBS (BioWhittaker, Cambrex, Walkersville, MD). To induce osteoclast differentiation, cells were cultured for 5 days in medium supplemented with 50 ng/ml of RANKL (PeproTech Inc., Rocky Hill, NJ), with changes of medium and RANKL every other day.

Bone marrow mononuclear cells (BMM) were collected from 2-week-old mice and cultured in  $\alpha$ -MEM medium (Invitrogen, Carlsbad, CA) with 10% nonheat inactivated FBS (BioWhittaker). To stimulate osteoclast differentiation, cells were cultured for 5 days in the presence of 50 ng/ml soluble RANKL (PeproTech Inc, Rocky Hill, NJ) and 25 ng/ml soluble M-CSF (PeproTech Inc.) with changes of medium, RANKL, and M-CSF every other day.

Human peripheral blood mononuclear cells (PBMCs) were isolated from PBS-diluted blood (1:1, vol/vol) by centrifugation on a Histopaque-1077 (Sigma-Aldrich, St. Louis, MO) density gradient. CD14<sup>+</sup> selection was performed with the Human CD14 Selection Cocktail (StemCell Technologies, Vancouver, Canada, catalog no. 18058). CD14<sup>+</sup> PBMCs were cultured for 4 days in  $\alpha$ -MEM with 10% FBS, supplemented with 180 ng/ml human RANKL (PeproTech Inc., Rocky Hill, NJ) and 150 ng/ml human M-CSF (PeproTech).

### REAL-TIME PCR

Total RNA was extracted using TRIzol Kit (TRIzol<sup>®</sup>, Invitrogen) and reverse transcribed with QuantiTect Reverse Transcription Kit (Qiagen, Valencia, CA). The resulting cDNA was used for PCR using SYBR-Green Master PCR mix (Bio-Rad, Hercules, CA). We used the following osteoclast specific gene primers:

$\beta$ -Actin (Forward): ACCGTGAAAAGATGACCCAG;  
 $\beta$ -Actin (Reverse): GTACGACCAGAGGCATACAG;  
TRAP (Forward): GCAGTATCTTCAGGACGAGAAC;  
TRAP (Reverse): TCCATAGTGAAACCGCAAGTAG;  
Cathepsin k (Forward): CTTAGTCTCCGCTCACAGTAG;

Cathepsin k (Reverse): ACTGGAACACCCACATCCTG;  
MMP9 (Forward): TCCGTGTCCTGTAAATCTGC;  
MMP9 (Reverse): TCCGTGTCCTGTAAATCTGC;  
SRC (Forward): ATGTGGAGCGGATGAACTATG;  
SRC (Reverse): GGCTGTGTATTCTGTGCTTC;  
SNX10 (Forward): GAACAATCGCCAGCATGTGCGAC;  
SNX10 (Reverse): ATGTCCTCGGAGTTCAGATGGC.

PCR was performed in triplicate on a Bio-Rad iCycler. All quantitations were normalized to the endogenous control  $\beta$ -Actin. The expression level difference (fold) between nondifferentiated cells and differentiated osteoclasts was presented by a semi log plot, as previously described [Yang et al., 2004].

### HISTOLOGY, IMMUNOHISTOCHEMISTRY, AND IMMUNOFLUORESCENCE

Embryos and 3-day-old mouse heads were fixed in 10% phosphate-buffered formaldehyde for 24 h, embedded in paraffin, and sectioned. Antigen detection on deparaffinized bone sections was performed according to standard protocols. Briefly, sections were incubated in a humidified chamber overnight at 4°C in primary antibody (rabbit anti-human SNX10 antibody, -HPA015605, Prestige Antibodies<sup>®</sup>, Sigma-Aldrich) at a 1:400 dilution. The following day, slides were washed 3 times for 10 min each in 1× PBS + 0.1% (vol/vol) Tween-20. Sections were then incubated for 1 h at room temperature with a biotinylated secondary antibody (dilution 1:200) in a humidified chamber. Slides were washed 3 times for 10 min each in 1× PBS and incubated with one drop of ABC solution (Ready-to-use Vectastain ABC Kit, Vector Laboratories, Inc., Burlingame, CA); incubated for 30 min at room temperature; washed 3 times for 5 min each in 1× PBS; and incubated for 2–10 min with DAB solution until the signal developed. Images were acquired with a LEICA DMLS optical microscope equipped with a LEICA DC 100 digital imaging system. For tartrate resistant acid phosphatase (TRAP) staining, adjacent tissue sections were deparaffinized in xylene and rehydrated in solutions containing decreasing concentrations of ethanol. Sections were then incubated with a solution of Naphthol AS-MX phosphate and Fast Red Violet LB Salt (Sigma-Aldrich), according to the manufacturer's instructions.

Immunofluorescence analysis was done following standard protocols. For SNX10 detection we used an anti-human SNX10 primary antibody (described above) and an Alexa red anti-rabbit secondary antibody (dilution 1:1,000, Invitrogen). For ER-specific staining we used a mouse IgG2b anti-protein disulfide isomerase (PDI) antibody (dilution 1:1,000, Invitrogen), and a FITC-conjugated anti-mouse secondary antibody (dilution 1:1,000). Cells were counterstained with DAPI (4',6-diamidino-2-phenylindole) prior to mounting on glass cover slips. Images were obtained with a Leica SP5X Laser Scanning Confocal Microscope.

### SUB-CELLULAR FRACTIONATION

Subcellular fractionation was done using the endoplasmic reticulum isolation kit (Sigma-Aldrich, ER0100). Briefly, RAW264.7 cells were cultured on a 10 cm plate for 5 days under differentiation conditions as described above. Differentiated osteoclasts were washed once in

PBS and incubated in 4 ml 1× hypotonic extraction buffer for 20 min at 4°C, to allow for cell swelling. After that, the hypotonic extraction buffer was removed and replaced with 2 ml 1× isotonic extraction buffer. The cells/isotonic buffer suspension was then homogenized with a Dounce Homogenizer (10 strokes) and subjected to differential centrifugation to separate the following three fractions: nuclear, mitochondrial, and rough ER. The concentration of protein was determined for all fractions. Equivalent amounts of protein were used for Western blot analysis.

#### MEASUREMENT OF SECRETED TRAP

RAW264.7 cells were cultured for 7 days on Osteo Assay Surface 24-well plates (Corning, # 3987) under differentiation conditions. This product is a crystalline calcium phosphate coating that mimics bone and can be used in osteoclast differentiation, for tartrate resistant acid phosphatase (TRAP) secretion, and surface resorption assays. Secreted TRAP measurement was performed with the Acid Phosphatase Assay Kit (Cayman Chemical, Ann Arbor, MI, # 10008051). This assay uses the chromogen para-nitrophenyl phosphate (pNPP) as a substrate for the enzyme, in a 2-step reaction. In the first step, AP dephosphorylates pNPP. In the second step, the phenolic OH-group is deprotonated under alkaline conditions to yield *p*-nitrophenolate, which gives a yellow color that can be measured at 405–414 nm. Twenty microliters of each supernatant were added to 48-well plates containing 10 µl of pNPP substrate solution and 20 µl of assay buffer. The plates were then incubated at 37°C for 20 min. The reactions were stopped by addition of 100 µl of 0.5 M sodium hydroxide. Optical absorbance was then measured at 405 nm on a plate reader against a standard curve of *p*-nitrophenol.

#### SNX10 SILENCING

RAW 264.7 cells were infected with a mix of five MISSION shRNA Lentiviral Particles targeting *snx10* (Sigma-Aldrich, SHCLNV-NM\_028035, TRCN0000105711, TRCN0000379561, TRCN0000105710, TRCN0000105712, and TRCN0000105713). Briefly, cells were cultured overnight in DMEM/10% FBS until 60–80% confluent. Infection was then carried out overnight in the presence of polybrene (5 µg/ml) at a multiplicity of infection (MOI) = 25. The following day, the culture medium was replaced with fresh medium without polybrene, and the cells were cultured for 48 h. Control cells were infected with an equivalent amount of scrambled *snx10* shRNA virus (Santa CRUZ, sc-108080). After that, cells were cultured in puromycin for 1 week. Puromycin resistant cells (cells infected with *snx10*-shRNA virus or *snx10*-scrambled virus) were pooled and used for further experiments. Pools of clones (instead of single clones of infected cells) are a representative sample of *Snx10*-silenced cell clones and were used to avoid clone specific bias.

To test whether *Snx10*-silencing affects resorption of differentiated osteoclasts we cultured RAW 264.7 on a 3D collagen matrix (Millipore ECM 675) and stimulated these cells with RANKL for 6 days to induce osteoclast differentiation. The differentiated cells were removed from the collagen matrix by incubating the plates with a collagenase solution (1,000 U/ml in PBS) for 30 min at 37°C. After complete digestion of the collagen, equal amounts of

differentiated cells (50,000 cells per well) were plated on 24-well osteologic plates (BD BioCoat™ Osteologic™) or 24 well plastic plates. Cells were maintained in differentiation medium plus RANKL. The following day cells were infected with 200 µl of a mixture of the five *Snx10* shRNA-viral particles in the presence of polybrene (5 µg/ml). Control cells were left uninfected or infected with 200 µl of *Snx10*-scrambled shRNA virus. Cells were then stimulated with RANKL to induce differentiation. After 4 days, cultures were stopped and analyzed for osteoclast gene expression and pit formation.

## RESULTS

### SNX10 EXPRESSION IS EXPRESSED BY OSTEOCLASTS IN VITRO AND IN VIVO

Using a genome-wide microarray screening approach, we studied differential gene expression in RANKL-stimulated monocytes (Table I) [Battaglini et al., 2002, 2004, 2008] and found *snx10* to be up-regulated during RANKL-induced osteoclastogenesis. SNX10 belongs to the sorting nexin (SNX) family of proteins that share a common feature: the PX domain [Worby and Dixon, 2002]. Multiple sequence alignment generated by MUSCLE version 3.6 [Edgar, 2004] (using option: –maxiters 2) demonstrated extensive sequence identity among vertebrate orthologues. Identity within the PX domains is 100% (Fig. 1).

PCR analysis confirmed a significant 7.5-fold increase in the expression of *Snx10* in osteoclasts derived from mouse bone marrow mononuclear cells (BMM). RANKL-induced expression of *Snx10* in osteoclasts paralleled that of TRAP (8.8-fold increase), Cathepsin K (23.1-fold increase), and MMP9 expression (2.8-fold increase). This indicates that RANKL induces *Snx10* expression in a manner similar to that of other well-known osteoclast genes (Fig. 2A). To study *Snx10* expression in vivo, we performed qPCR analysis from RNA derived from 2-week-old mice femora and calvariae (tissues rich in mature osteoclasts) and compared gene expression levels to osteoclast precursors in the bone marrow. The in vivo results (Fig. 2B) demonstrate an increase in *Snx10* expression (ninefold) in femur (containing mature osteoclasts), compared with expression seen in BMM cells (which includes osteoclast precursors). The pattern was similar to that found in RANKL-induced osteoclasts. SNX10 expression was 32.4-fold higher in calvariae compared with

TABLE I. Affymetrix Screening: Summary of Results

Affymetrix probe set	Gene name	<i>P</i> -value (RAW)	<i>P</i> -value (BMC)
98859_at	TRAP	0	0
160901_at	c-fos	0	0
160406_at	Cathepsin K	0	0
99957_at	MMP9	0	0
94556_at	SNX10	0	0

We conducted a microarray genome-wide screening in RAW 264.7 cells as well as in normal BMC stimulated with RANKL. Unstimulated cells were used as controls. Only genes whose expression was upregulated in both cellular systems were selected for further analysis. The *P*-value calculated for each gene indicates the probability of an RANKL-induced increase in gene expression. A *P*-value near or equal to zero indicates very high probability. Among the top genes identified in this screening, there are several well-known osteoclast-specific genes (TRAP, c-fos, cathepsin K, MMP-9). Finally, we also identified clone 96481\_AT, which contains part of SNX10 and whose expression was upregulated in RANKL-stimulated RAW 264.7 and BMC cells.

Human	1	-----MFPEQK-----EEFV <b>SVVVRDPRIQKEDFWH</b>	27
Mouse	1	-----MFPEQK-----EEFV <b>SVVVRDPRIQKEDFWH</b>	27
Chicken	1	-----MTPKHEK-----QEFV <b>TVLVRDPRTQKEDSWH</b>	27
ZebraFish	1	-----MDNTSFEK-----REFI <b>SVVVRDPQVHKEDFWH</b>	28
Human	28	<b>SYIDYEICHTNSMCFMTKTSVRRRYREFVWLRQRLQSNALLVQLPELP</b>	77
Mouse	28	<b>SYIDYEICHTNSMCFMTKTSVRRRYREFVWLRQRLQSNALLVQLPELP</b>	77
Chicken	28	<b>SYIDYEIFHTNSMCFTRKTSVRRRYREFVWLRQRLQSNALLVQLPELP</b>	77
ZebraFish	29	<b>TYISYEICLHTNSMCFRKKTSVRRRYSEFVWLRHKLQDNALLIELPKLP</b>	78
Human	78	<b>SKNLFFNMNRQHVDQRRQGLEDFLRKVLQNALLLSDSSLHLFLQSHLNS</b>	127
Mouse	78	<b>SKNLFFNMNRQHVDQRRQGLEDFLRKVLQNALLLSDSSLHLFLQSHLNS</b>	127
Chicken	78	<b>SKTPFFNMNPHHVDHRRQGLEDFLEKILQNALLLSDSRLHLFLQTLQSP</b>	127
ZebraFish	79	<b>PWNPFNLNNEFHITQRMQGLQFLEAVLQTPLLLSDSRLHLFLQSLSI</b>	128
Human	128	EDIEACVSGQTKYSVEEAIHKFALMNRFPVEEDEEGKKE-NDIDYDSES-	175
Mouse	128	EDIEACVSGQTKYSVEEAIHKFALMNRFPVEEDEEGKKE-AEVEYDSES-	175
Chicken	128	EDMEACVCGQTKYSVADAIQKFAFLNRRFPVEEERKKGKGRNDADSDSES-	176
ZebraFish	129	AKMDACAQGHHTYTAQAIQRCGG-EARFPVEEQHQEDSKTCCDSDCDST	177
Human	176	SSSGLGHS-----SDDSSSHGCKVNTAPQES-----	201
Mouse	176	SSSGLGHS-----SDDSSSHGCKTSPALQES-----	201
Chicken	177	SSSGLG-P-----SDDSSICGCKASLASEES-----	201
ZebraFish	178	TSSGLGCSIEPATLVEQDLSHNERFAHEFQATNPEAELCSSLSSPHGHS	227
Human	--	--	--
Mouse	--	--	--
Chicken	--	--	--
ZebraFish	228	VI 229	--

Fig. 1. Sequence alignment of SNX10. SNX10 from vertebrates displays a high degree of identity (over 90%). The PX domain, from position 12 to 109 (shaded), is 100% conserved across species.

osteoclast precursors. These results suggest that *Snx10* is also expressed by osteoclasts in bone.

To visualize in situ expression of *Snx10* in vivo, we performed immunohistochemical analysis of mouse embryo sections at 16.5, 17.5, 18.5 days-post-coitum (dpc), and of 3-day-old mice. We chose these stages because of the high level of active osteoclast differentiation. SNX10 expression was clearly detected in calvariae and developing teeth (Fig. 3). There is no staining in adjacent IgG control-sections (data not shown). Adjacent sections stained for TRAP (Fig. 3) show co-localization of TRAP activity and SNX10

protein expression, demonstrating osteoclastic localization of SNX10. Taken together, these results confirm that SNX10 is expressed in osteoclasts.

#### SUB-CELLULAR LOCALIZATION

To study the sub-cellular localization of SNX10 we conducted confocal immunofluorescent microscopic analysis of osteoclasts derived from M-CSF/RANKL-stimulated human CD14<sup>+</sup> peripheral blood mononuclear cells (hPBMCs), using a SNX10 specific antibody. These results (Fig. 4, top) suggest *Snx10* nuclear and

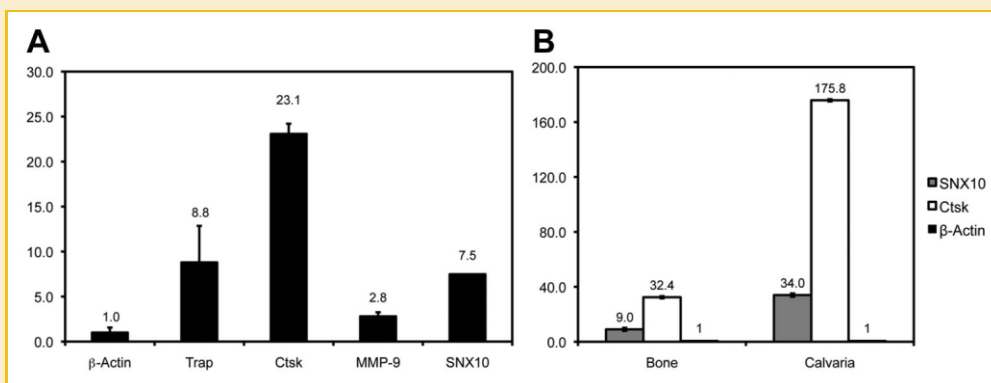


Fig. 2. SNX10 expression: mRNA. A: qPCR analysis of RNA derived from mouse bone marrow mononuclear cells (BMM) and osteoclasts (OC) shows up-regulation of SNX10 expression in OC. The numbers over the error bars indicate relative levels of SNX10 mRNA expression (OC/BMM, standardized for  $\beta$ -actin) and are the average of three independent amplifications. The expression pattern of SNX10 is similar to that of the OC-specific genes TRAP, Cathepsin K, and MMP9. B: qPCR analysis of RNA derived from mouse bone marrow mononuclear cells (BMM), 2-week-old mouse bones (femur) and calvariae, shows up-regulation of SNX10 expression in both femur and calvaria. The numbers over the error bars indicate relative levels of *snx10* mRNA expression (Bone/BMM and Calvaria/BMM, standardized for  $\beta$ -actin) and are the average of three independent amplifications.



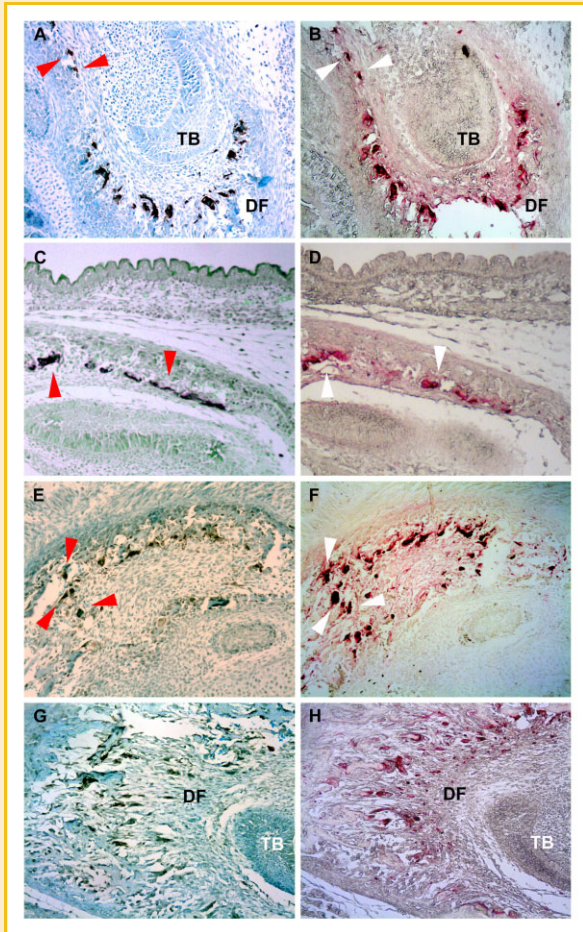


Fig. 3. SNX10 expression: protein. Immunohistochemical analysis of mouse histological sections using a SNX10-specific antibody shows expression in (A) 16.5 dpc maxillary incisor, (C) 17.5 dpc calvaria, (E) 18.5 dpc nasale bone and (G) 3-day-old mandibular incisor. Adjacent sections were TRAP-stained (B, D, F, and H, respectively). SNX10 expression co-localizes with TRAP staining. TB, tooth bud; DF, dental follicle (indicated by red and white arrows).

endoplasmic reticulum (ER) localization in human osteoclasts. We also conducted cell fractionation of RAW264.7-derived osteoclasts, followed by Western blot analysis using a Snx10-specific antibody. The results (Fig. 4, bottom) confirm expression of Snx10 in both ER and nuclear fractions.

### Snx10 IS REQUIRED FOR OSTEOCLAST DIFFERENTIATION AND RESORPTION ACTIVITY

*Snx10* is expressed predominantly in osteoclasts and we hypothesized that *Snx10* activity was required for osteoclast differentiation and/or function. To test this hypothesis we infected RAW 264.7 cells with a Snx10-shRNA containing virus and stimulated them with RANKL to induce osteoclast differentiation. Control cells were left uninfected (negative control) or infected with a Snx10 scrambled shRNA-containing virus. Densitometric analysis of the Western blot (using Image J) showed a significant 90% reduction in Snx10 protein expression in Snx10-shRNA infected cells (Fig. 5A,B). q-PCR analysis also revealed that *snx10* silencing inhibited expression of

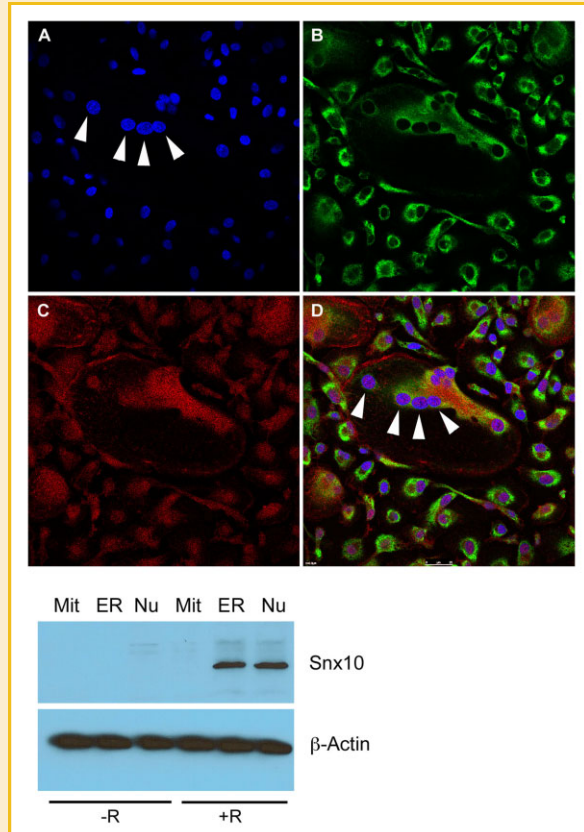


Fig. 4. SNX10 subcellular localization. (top) Osteoclasts derived from M-CSF/RANKL-stimulated human CD14<sup>+</sup> peripheral blood mononuclear cells were fixed and stained with DAPI to indicate the nucleus, with an anti-protein disulfide isomerase (PDI) antibody to indicate the ER, and an anti-SNX10 antibody. The three confocal images show (A) the nuclei, (B) the ER, and (C) SNX10 for the same multinucleated osteoclast. The superimposed image (D) shows co-localization of SNX10 with nuclei (white arrows) and also partially with the ER. (bottom) Western blot analysis of subcellular fractions shows Snx10 expression in RANKL-stimulated cells (+R) but not in un-stimulated control cells (-R). Snx10 is expressed in the endoplasmic reticulum (ER), nucleus (N) but in mitochondria (Mit).

TRAP, Cathepsin K and MMP-9 in RANKL induced osteoclast precursors (Fig. 5B). The formation of TRAP<sup>+</sup> multinucleated cells and surface resorption activity was abolished by *snx10* silencing (Fig. 5C). RAW264.7 cells growing on calcium phosphate secrete TRAP into the medium when stimulated with RANKL. The secretion of TRAP was reduced by 50% following *snx10* silencing (Fig. 5D). Together, these results indicate that *snx10* expression is required for osteoclast differentiation and resorption.

### Snx10 SILENCING DOES NOT INHIBIT PIT FORMATION BY DIFFERENTIATED OSTEOCLASTS

The inhibitory effect of Snx10 silencing on pit formation could be due to inhibition of osteoclast formation or inhibition of activity of differentiated osteoclasts. In order to clarify this point, we induced osteoclast differentiation of RAW264.7 cells and then infected differentiated osteoclasts with a Snx10 shRNA-virus before plating them on calcium phosphate coated plates. We found a significant

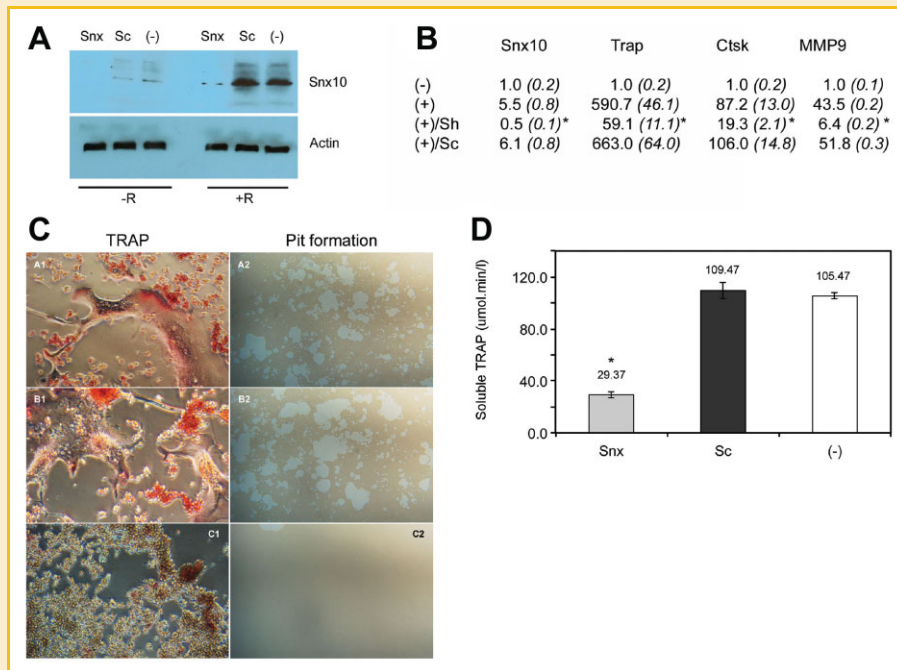


Fig. 5. *snx10* silencing inhibits osteoclast differentiation. A: RAW 264.7 cells were infected with a mix of *snx10*-specific shRNA virus. Western Blot analysis of proteins derived from cells infected with a *snx10*-specific shRNA virus (Snx) shows a significant reduction in the expression of *snx10*, compared to cells infected with a *snx10*-scrambled shRNA virus (Sc) or uninfected control cells (-). Image analysis shows a knockdown efficiency of >90%. B: Relative expression of osteoclast-specific genes (expression in Sc infected cells/expression in *snx10* shRNA infected cells) by qPCR analysis. Experiments were done in triplicates and expressed as Mean (SD) (\* $P < 0.05$ ). C: *snx10* shRNA-infected RAW 264.7 cells fail to form TRAP<sup>+</sup> cells (C1) and to form resorption pits (C2) on a calcium phosphate matrix. Cells infected with a scrambled virus form TRAP<sup>+</sup> cells (A1) and numerous resorption pits (A2). Uninfected cells form TRAP positive cells and resorption pits (B1 and B2). D: *snx10* shRNA-infected RAW 264.7 cells stimulated with RANKL secrete 26% TRAP, compared with control cells ( $P < < 0.001$ ) infected with a scrambled virus (Sc) or uninfected (-). This plot is representative of 3 independent experiments. [Color figure can be seen in the online version of this article, available at <http://wileyonlinelibrary.com/journal/jcb>]

reduction in Snx10 protein (Fig. 6A, ~50%) and RNA (Fig. 6B, ~80%). We did not observe significant differences in either soluble secreted TRAP (Fig. 6C) or pit formation (Fig. 6D) in Snx10-shRNA infected cells. These results suggest that Snx10-silencing inhibits osteoclast formation. Notably, while expression of early markers of osteoclast differentiation TRAP and Ctsk is not inhibited by Snx10 silencing, expression of MMP-9 is significantly reduced (87%). This reduction is equivalent (88%) to the inhibition observed when Snx10 silencing was done in differentiating osteoclasts precursors (Fig. 5B). RANKL-stimulated RAW 264.7 cells sequentially express TRAP, Ctsk, and MMP-9 (in that order) [Battaglini et al., 2002]. These results suggest that Snx10 silencing affects a later step in osteoclast formation, after TRAP and Ctsk expression but before MMP-9 expression.

## DISCUSSION

We detected up-regulation of *snx10* during the course of a genome-wide screening performed to identify genes induced by RANKL stimulation of osteoclast precursors. SNX10 expression in osteoclasts has been previously reported [Hecht et al., 2007] in a study comparing expression profiles of wild-type and *Runx2*<sup>-/-</sup> mouse embryonic bones. However, the authors did not explore a possible role of *snx10* in osteoclast formation/function and listed it as a gene

with a known function in other contexts, but no known role in skeletal development. Our results expand those of Hecht et al. by demonstrating mRNA and protein expression of Snx10 during RANKL-induced osteoclast differentiation in vitro and in vivo. Confocal microscopy analysis suggests that *snx10* localizes to the ER and nucleus in differentiated human osteoclasts. Western Blot analysis of subcellular fractions confirms this observation. More important, our results show that *snx10* is essential for RANKL-induced osteoclast formation and function. Given the high degree of sequence conservation among Snx10 vertebrate orthologues, we anticipate that all the orthologues will exhibit a similar restricted expression pattern and a similar function. Since osteoclasts are present only in vertebrates, the Snx10 family also appears to have evolved in parallel with vertebrates.

Regarding SNX10 subcellular localization, our results do not completely agree with a previous report that describes SNX10 colocalization with endosome markers [Qin et al., 2006]. However, the Qin study describes the localization of a *transfected* Snx0 fused to a GFP or FLAG epitope, not the endogenous protein. Over-expressed fusion proteins may localize to a compartment different than that of native proteins due to the presence of the fused tag. This may explain the differences detected in subcellular localization. Most published studies have shown SNXs to be hydrophilic molecules that localize to the cytoplasm and have the potential for membrane association either through their lipid binding PX domains or through protein-

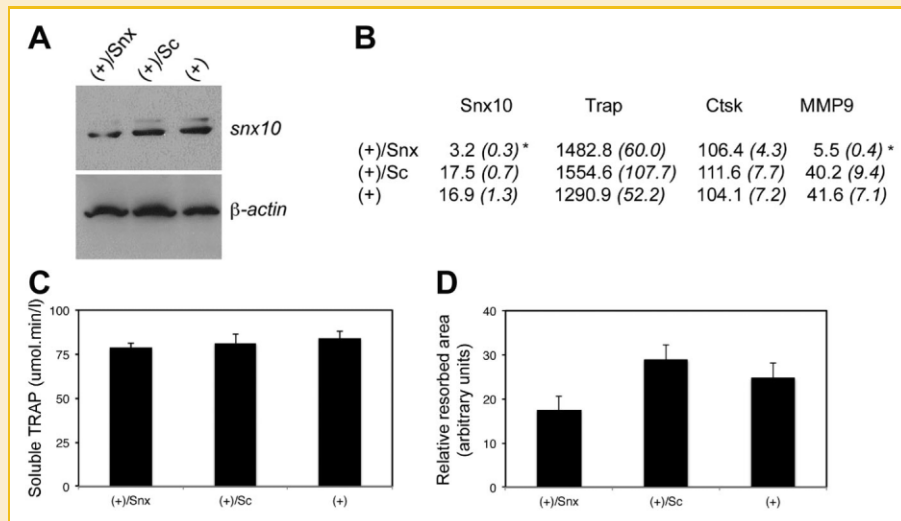


Fig. 6. *snx10* silencing in differentiated osteoclasts does not affect resorption activity. A: RAW 264.7 cells were induced to differentiate on a collagen matrix and subsequently infected with a mix of *snx10*-specific shRNA virus. Western Blot analysis of proteins derived from cells infected with a *Snx10*-specific shRNA virus (+/Snx) shows a significant reduction in the expression of *snx10*, compared to cells infected with a *Snx10*-scrambled shRNA virus (+/Sc) or uninfected control cells (+). Image analysis shows a knock-down efficiency of ~50%. B: Relative expression of osteoclast-specific genes (expression in Sc infected cells/expression in *snx10* shRNA infected cells) by qPCR analysis. Experiments were done in triplicates and expressed as Mean (SD) (\* $P < 0.05$ ). C: *snx10* shRNA-infected RAW 264.7 cells stimulated with RANKL secrete the same amount of TRAP, compared with control cells (\* $P < 0.001$ ) infected with a scrambled virus (+/Sc) or uninfected (+). This plot is representative of three independent experiments. D: *snx10* shRNA-infected osteoclasts (+/Snx) and osteoclasts infected with a scrambled *snx10* shRNA (+/Sc) can form resorption pits on calcium phosphate. There are no statistically significant differences in the areas resorbed by (+/Snx), (+/Sc) and uninfected (+) osteoclasts.

protein interactions with membrane-associated protein complexes [Worby and Dixon, 2002]. For instance, SNX3 was reported to co-localize with EEA1 (an effector of the small GTPase Rab5) in early endosomes [Pons et al., 2008]. SNX6, another SNX family member, was reported to localize to the cytoplasm but also to translocate to the nucleus [Ishibashi et al., 2001]. Our data demonstrate dual localization of *Snx10* in human osteoclasts. Understanding the functional implications of this observation will require further studies.

Vesicular transport along microtubules is essential for resorbing osteoclasts. Rab3D, a member of the GTPase family, regulates post-trans-Golgi network trafficking that is required for the maintenance of the ruffled border membrane [Pavlos et al., 2005]. Tctex-1, a Rab3D-binding protein, is co-expressed with Rab3D on secretory vesicles in bone-resorbing osteoclasts. Silencing of Tctex-1 causes Rab3D to mislocalize thereby impairing osteoclastic bone resorption [Pavlos et al., 2011]. This inhibition of osteoclast activity by Tctex-1 silencing is similar to that observed in osteoclasts derived from Rab3D-deficient mice [Pavlos et al., 2005], indicating that Tctex-1 may be part of the Rab3D vesicle transport machinery. Finally, the authors speculate that Tctex-1 might be recruited to Rab3D-expressing vesicles in osteoclasts during resorption, serving as a molecular adaptor linking Rab3D vesicles to microtubules and connecting membrane and microtubule transport during bone resorption. Our results in differentiated osteoclasts show *Snx10* expression in a pattern similar to that of Tctex-1, suggesting that *Snx10* role in vesicular transport could be mediated by a similar mechanism. However, important differences should be pointed out. While Tctex-1 is expressed in osteoclast precursors and is upregulated early on during RANKL-induced osteoclast differentia-

tion (day 1, [Pavlos et al., 2011]) *Snx10* is not expressed in osteoclast precursors. Tctex-1 silencing inhibits osteoclast resorption but not osteoclast formation. *Snx10* silencing, on the other hand, inhibits osteoclast formation but does not affect resorption activity of previously differentiated osteoclasts.

Finally, SNX10 has been shown to induce the formation of vacuolae in transfected 293 cells [Qin et al., 2006]. More recently, the same authors reported that SNX10 interacts with the V-ATPase complex and that this interaction regulates vesicular trafficking [Chen et al., 2011]. This raises the possibility that *Snx10* could interact with the osteoclast ATPase and that such interaction is required for osteoclast formation and/or activation. Additional work is required to confirm this hypothesis.

SNXs share homology with PX-containing yeast proteins Vps1, Vps5, and Vps17, all involved in vacuole sorting, suggesting that SNXs can regulate membrane trafficking [Qin et al., 2006]. There are roughly 30 members in the SNX family. Only a few members have been characterized so far. They all appear to function in cargo-sorting in the endosomes. The functional characterization of most SNXs, however, remains to be done [Carlton et al., 2004, 2005]. SNX10 over-expression induced giant vacuoles in mammalian cells [Qin et al., 2006]. Moreover, the vacuolization process was inhibited by Brefeldin A. Taken together, these results suggest that *Snx10* activity is involved in the regulation of membrane trafficking and endosome homeostasis.

Our results clearly indicate a role for *Snx10* in the regulation of osteoclast formation and function in vitro. These studies suggest that *Snx10* could play a role in bone homeostasis in vivo. Since vesicular trafficking is essential for osteoclast formation and activity and *Snx10* is involved in intracellular vesicular trafficking,



this gene may be involved in the development of human bone diseases; either osteopetrosis or osteoporosis. We expect this work to provide the foundation for future studies of Snx10 in the regulation of bone mass under normal and pathological conditions in humans, as well as explore a potential new target for anti-resorptive therapies.

## ACKNOWLEDGMENTS

The authors thank Justine Dobeck for her invaluable expertise in histological analysis and Cathy Wolff for assistance with manuscript preparation and editing.

## REFERENCES

- Battaglino R, Fu J, Spate U, Ersoy U, Joe M, Sedaghat L, Stashenko P. 2004. Serotonin regulates osteoclast differentiation through its transporter. *J Bone Miner Res* 19:1420–1431.
- Battaglino R, Kim D, Fu J, Vaage B, Fu XY, Stashenko P. 2002. c-myc is required for osteoclast differentiation. *J Bone Miner Res* 17:763–773.
- Battaglino RA, Pham L, Morse LR, Vokes M, Sharma A, Odgren PR, Yang M, Sasaki H, Stashenko P. 2008. NHA-oc/NHA2: A mitochondrial cation-proton antiporter selectively expressed in osteoclasts. *Bone* 42:180–192.
- Carlton J, Bujny M, Peter BJ, Oorschot VM, Rutherford A, Mellor H, Klumperman J, McMahon HT, Cullen PJ. 2004. Sorting nexin-1 mediates tubular endosome-to-TGN transport through coincidence sensing of high-curvature membranes and 3-phosphoinositides. *Curr Biol* 14:1791–1800.
- Carlton J, Bujny M, Rutherford A, Cullen P. 2005. Sorting nexins—Unifying trends and new perspectives. *Traffic* 6:75–82.
- Chen Y, Wu B, Xu L, Li H, Xia J, Yin W, Li Z, Li S, Lin S, Shu X, Pei D. 2011. A SNX10/V-ATPase pathway regulates ciliogenesis in vitro and in vivo. *Cell Res*.
- Coxon FP, Taylor A. 2008. Vesicular trafficking in osteoclasts. *Semin Cell Dev Biol* 19:424–433.
- Edgar RC. 2004. MUSCLE: Multiple sequence alignment with high accuracy and high throughput. *Nucleic Acids Res* 32:1792–1797.
- Hecht J, Seitz V, Urban M, Wagner F, Robinson PN, Stiege A, Dieterich C, Kornak U, Wilkening U, Brieske N, Zwingman C, Kidess A, Stricker S, Mundlos S. 2007. Detection of novel skeletogenesis target genes by comprehensive analysis of a Runx2(–/–) mouse model. *Gene Expr Patterns* 7:102–112.
- Ishibashi Y, Maita H, Yano M, Koike N, Tamai K, Ariga H, Iguchi-Arigo SM. 2001. Pim-1 translocates sorting nexin 6/TRAF4-associated factor 2 from cytoplasm to nucleus. *FEBS Lett* 506:33–38.
- Pavlos NJ, Cheng TS, Qin A, Ng PY, Feng HT, Ang ES, Carrello A, Sung CH, Jahn R, Zheng MH, Xu J. 2011. Tctex-1, a novel interaction partner of Rab3D, is required for osteoclastic bone resorption. *Mol Cell Biol* 31:1551–1564.
- Pavlos NJ, Xu J, Riedel D, Yeoh JS, Teitelbaum SL, Papadimitriou JM, Jahn R, Ross FP, Zheng MH. 2005. Rab3D regulates a novel vesicular trafficking pathway that is required for osteoclastic bone resorption. *Mol Cell Biol* 25:5253–5269.
- Pons V, Luyet PP, Morel E, Abrami L, van der Goot FG, Parton RG, Gruenberg J. 2008. Hrs and SNX3 functions in sorting and membrane invagination within multivesicular bodies. *PLoS Biol* 6:e214.
- Qin B, He M, Chen X, Pei D. 2006. Sorting nexin 10 induces giant vacuoles in mammalian cells. *J Biol Chem* 281:36891–36896.
- Baron R, Horne WC. 2005. Regulation of osteoclast activity. *Bone Resorption* 2.
- Stenbeck G, Horton MA. 2004. Endocytic trafficking in actively resorbing osteoclasts. *J Cell Sci* 117:827–836.
- Worby CA, Dixon JE. 2002. Sorting out the cellular functions of sorting nexins. *Nat Rev Mol Cell Biol* 3:919–931.
- Yang J, Mani SA, Donaher JL, Ramaswamy S, Itzykson RA, Come C, Savagner P, Gitelman I, Richardson A, Weinberg RA. 2004. Twist, a master regulator of morphogenesis, plays an essential role in tumor metastasis. *Cell* 117:927–939.